2 Thermogravimetry

P.J. Haines

2.1 Introduction

The measurement of the mass of a sample is often one of the earliest quantitative experiments we do. Every day, many portions of foods, pharmaceuticals, containers, chemicals, polymers or engineering parts are weighed and recorded. The extension of this simple technique into analysis provides the discipline of *gravimetric analysis*. This has been defined [1] as 'quantitative analysis by weight' and is the process of isolating and weighing an element or a definite compound of the element in as pure a form as possible. Gravimetric experiments to determine water of crystallisation, and to study oxidation and reduction, are used to teach the principles of stoichiometry, formulae and analysis. Many gravimetric techniques involve a reaction to produce a definite compound and then heating it to convert to a stable material of known composition. For example, bismuth may be precipitated as a cupferron complex, but must then be ignited 'strongly' to give the stable oxide Bi_2O_3 [1].

The samples that the analyst is given need to be studied in the form 'as received' and frequently this neither is a definite compound nor is it pure! While we shall try to perform quantitative analysis, the answers will often be very dependent on the treatment regime and the method of analysis. As a practical example, the moisture content of a sample of soil may be measured by drying below 100 °C and its content of organic materials by igniting at around 500 °C [2].

If we can follow all the effects of heat on the changing mass of the sample, we should be able to extract information on the stages of analysis and on the temperatures needed to bring each stage to completion.

Measurement of *mass* on a balance is done by the process of weighing. That is, a balance compares the unknown mass with a standard mass by comparing their *weights*, which have the units of *force* (newtons) and the magnitude of *mass times gravitational acceleration*. The mass of a body stays *constant*, but the weight will alter if the acceleration acting on the body alters.

2.2 Historical

The origins of thermogravimetry have been fully documented by Duval [3], Keattch and Dollimore [4] and Wendlandt [5]. The most significant

P. J. Haines, *Thermal Methods of Analysis*

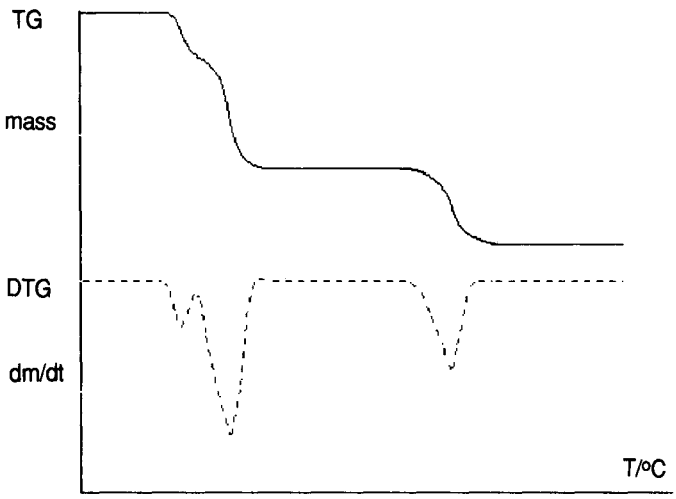

Figure 2.1 Typical TG (solid) and DTG (dashed) curves.

contribution was made by Honda [6] in 1915 who used a lever-arm balance fitted with an electrical furnace to investigate manganese oxysalts. Simple experimental apparatus has been described which uses modified manual analytical balances and controlled electric furnaces [7]. The Chevenard thermobalance was the first to record weight changes automatically using a photographic method. This was used extensively from 1936 by Duval and others [8].

The development of the electronic microbalance [9] allowed smaller samples and furnaces to be used, and work to be carried out in controlled atmospheres and in vacuum.

2.3 Definition of thermogravimetry

Thermogravimetry (TG) [10] is a technique in which the *mass* of the sample is monitored against time or temperature while the temperature of the sample, in a specified atmosphere, is programmed.

It should be recognised that several manufacturers and users prefer to call this technique *thermogravimetric analysis* (TGA). This avoids confusion with the glass transition temperature, T_g. The apparatus is called a *thermobalance*, or less frequently, a thermogravimetric analyser.

In order to enhance the steps in the thermogravimetric curve, the *derivative thermogravimetric* (DTG) trace is frequently drawn. Remember that this is the plot of the *rate of mass change, with time*, d*m*/d*t*.

2.4 Apparatus

As with most thermal analysis systems, the thermobalance has four major parts:

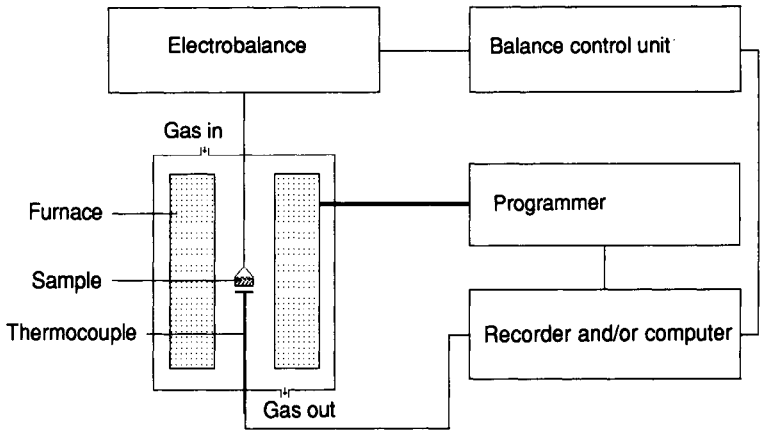

Figure 2.2 Schematic diagram of thermobalance system.

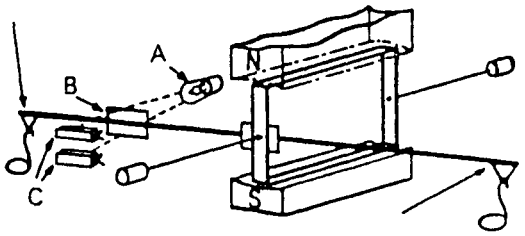

Figure 2.3 Schematic of a microbalance: A, lamp; B, shutter; C, photocells. (Courtesy CI Electronics Ltd.)

- the electrobalance and its controller
- the furnace and temperature sensors
- the programmer or computer
- the recorder, plotter or data acquisition device.

2.4.1 *The balance*

The balance used in many of the commercial apparati is a modified electronic microbalance. One example is shown in Figure 2.3. The light-weight arm is pivoted about an electrical coil suspended in a magnetic field. The position of the arm is measured by an optical sensor and any deflection

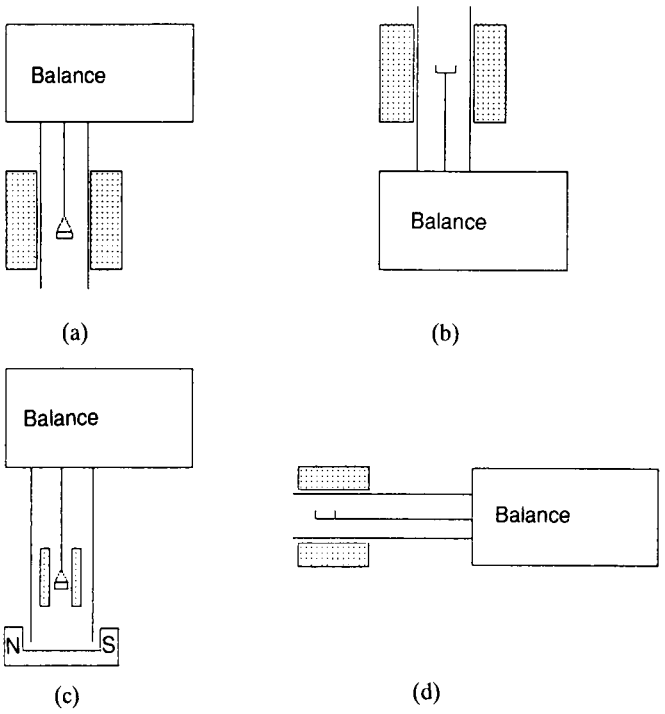

Figure 2.4 Arrangements of thermobalances, showing the furnace (shaded), sample position and casing: (a) and (c) suspended; (b) top-loading; (d) horizontal. The magnet position for Curie point calibration is shown in (c). (After [11].)

causes a current to be supplied to the coil which restores it to the 'null' position. This is important for maintaining a constant position of the sample in the same zone of the furnace. The sample suspended into the furnace from one arm of the balance is counterbalanced by a tare, either electrically applied to the coil or added to the reference pan. The balances will often give a resolution of 1 μg or better, and sample sizes range from a few milligrams up to 30 g. With this very high sensitivity, freedom from vibration is essential.

Several different arrangements of the balance and furnace are possible, as shown in Figure 2.4 [11], and the geometry may affect the results obtained.

The difficulties that may affect the operation of a balance used in conjunction with a furnace are most important. The presence of corrosive or oxidising gases near the balance mechanism is most undesirable, and the balance enclosure is often *purged* with an inert gas such as nitrogen at room temperature. Problems with static electricity, which can cause the attraction of the sample pan onto the glass enclosure, may be overcome by coating the surfaces with a conducting film or use of antistatic spray.

The movement of the gas surrounding the sample due to convection may cause noise and affect the observed mass. This may be reduced by introducing baffles within the sample enclosure. Usually experiments are conducted in a flowing atmosphere, and suitable design reduces convective effects.

Thermomolecular flow may occur when the balance is operated at low pressure [12]. If the sample or its suspension or the counterpoise experience temperature gradients when the pressure is low and the mean free path is comparable to the dimensions of the apparatus, the flow of gas molecules causes an apparent mass change.

With a temperature difference of 100 K, and a pressure of 10^{-1} torr, the effect can be as much as 100 μg.

When samples of large volume must be used, there is an effect due to Archimedes' Principle that 'when a body is immersed in a fluid it experiences an upthrust equal in magnitude to the weight of fluid displaced' [13]. If the volume of sample plus sample holder is V m^3 and the pressure p Pa, then the *mass* of an ideal gas of molar mass M displaced at temperature T will be:

$$m = MpV/RT$$

As the sample is heated, so the density of the gas decreases, while the density of the solids hardly changes. Therefore the upthrust will decrease, and the sample will *apparently gain* in measured mass.

As an example, consider a sample plus crucible of volume 1 cm^3, that is 10^{-6} m^3, at atmospheric pressure, approximately 10^5 Pa of nitrogen gas (M = 0.028 kg). If the molar gas constant R is 8.314 J/(K mol) then the buoyancy will change by about 0.8 mg between 300 K and 1000 K, so there will be an apparent weight *gain* of 0.8 mg.

There are several ways to compensate for this effect. Firstly, we may run a 'blank' buoyancy curve with an inert sample of similar volume and subtract this curve from the experimental curve for our sample.

Secondly, the use of very small samples and crucibles will reduce the effect. If the volume is reduced to 2.8×10^{-3} cm^3, equivalent to 10 mg of MgO, then the apparent gain in mass is only 2.2 μg.

Thirdly, if we use a twin furnace system as shown in Figure 2.5 [14,15] where a counterpoise of similar volume is heated at the same time, the effects largely cancel.

Thermogravimetry in very corrosive atmospheres may be carried out using a magnetically suspended balance [16,17], as shown in Figure 2.6. An electromagnet suspended from the microbalance holds a glass-encased permanent magnet in the measuring cell. The sample in the furnace is connected by a suspension wire to the permanent magnet and each mass change is transmitted back without contact. This allows the use of very reactive atmospheres, or of samples which produce corrosive or toxic products, without their coming into contact with the balance mechanism.

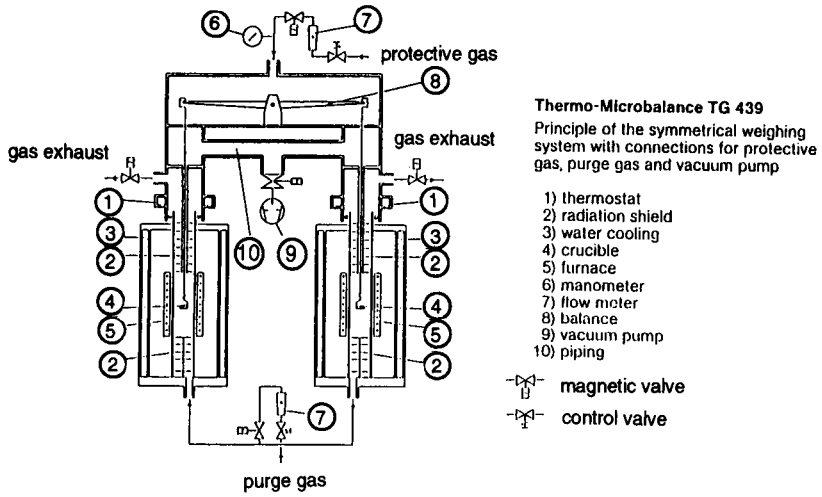

Figure 2.5 Diagram of a symmetrical thermo-microbalance. (Courtesy Netzsch-Mastermix Ltd [15].)

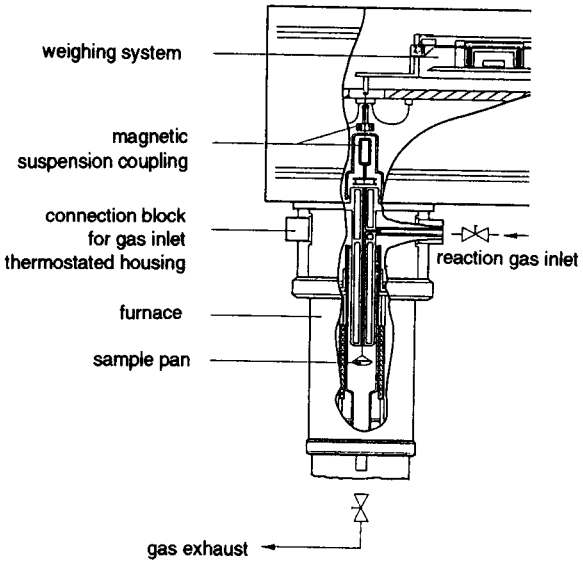

Figure 2.6 Diagram of a magnetic suspension thermo-microbalance. (Courtesy Netzsch-Mastermix Ltd [17].)

2.4.2 *Furnace*

The furnaces used are generally non-inductively wound electrical resistance heaters, although infrared and microwave heating have been suggested. The furnace and balance arrangements are shown in Figure 2.4. The most important features needed from the furnace are listed below:

1. The furnace should have a zone of uniform temperature which is considerably longer than the sample plus holder. This is much easier to achieve with small samples and holders.
2. The heat from the furnace must not affect the balance mechanism. Often baffles are placed between the two to reduce transfer of heat.
3. The furnace should be capable of rapid response and a range of heating and cooling rates, and should be capable of heating to temperatures well above those of interest. Rapid cooling is also most useful when a quick 'turn round' time is needed when many samples must be run.
4. The furnace lining should be inert at all temperatures used. A tube of ceramic such as alumina or mullite, or, for lower temperatures, silica glass may surround the sample, or in some cases, furnace and sample.

2.4.3 *Programmer*

The furnace temperature is measured by a thermocouple, generally platinum–platinum 13% rhodium, which is most suitable up to 1600 °C, is chemically fairly inert but has a fairly low output of about 8–12 μV/K. Another thermocouple often used is chromel–alumel which is suitable to 1100 °C, has a larger response of about 40 μV/K, but is more easily oxidised.

The signal from the furnace (or control) thermocouple is transmitted to the programmer and the temperature it represents is compared with that required by the programme set by the operator. If the temperature is too low, the system must respond by supplying more power to the furnace, and, if too high, by reducing the power. The response times of the controller and of the furnace govern the thermal lag of the instrument and hence the range of heating rates that is achievable. A slow response programmer controlling a very large furnace may only allow heating rates below 10 K/min, whereas a small mass furnace and a fast controller will allow rates up to 100 K/min [18].

2.4.4. *Samples*

Thermogravimetry is most frequently carried out on solids. The sample should be obtained in an approved way [19,20] so that it provides a

meaningful analysis. This is easy with pure, homogeneous compounds, but very difficult with large samples which may differ from one region to another. Procedures such as 'coning and quartering' of a finely ground sample may give better reproducibility, but often the very differences that we observe between samples are significant. One region of a sample may be more porous, or more easily oxidised, or have a higher moisture content than the bulk of the sample. Crystalline samples may behave differently from fine powders, especially where surface reactions are involved. It is also very often difficult to produce a fine powder from samples such as thermoplastics.

Samples should ideally be small, powdered and spread evenly in the crucible. Typical thermogravimetric runs might be done under the conditions given below.

Sample:	Calcium oxalate monohydrate
Crucible:	Platinum pan
Rate:	10 K/min
Atmosphere:	Nitrogen, 20 cm^3/min
Mass:	10.5 mg

Other examples are given later in the book.

2.4.5 *Temperature calibration*

In order that the balance shall operate with as little interference as possible, the sample temperature is often measured by a thermocouple placed near to, but *not in contact with* the sample.

Sample temperature thermocouples are generally of the same types used for furnaces, but frequently rather smaller and more delicate, since they are nearer the sample and the products of reactions.

The temperature measured by a thermocouple which is not in contact with the sample must be subject to a thermal lag which could be several degrees. Unless the experiment is carried out isothermally on a very small sample, this lag will vary with temperature and with the reactions proceeding, the furnace atmosphere, the heating rate and the geometry of the system. It is very important to calibrate the thermobalance in conditions which reproduce those which will be used in actual experiments, and to be able to reproduce the conditions on a variety of instruments. A survey was carried out by ICTAC of the most appropriate method of temperature calibration of thermobalances and concluded that a sharp, reproducible physical change would give the best results. The materials selected are metals and alloys which are ferromagnetic at low temperature, but which lose their ferromagnetism at a well-defined Curie point [21].

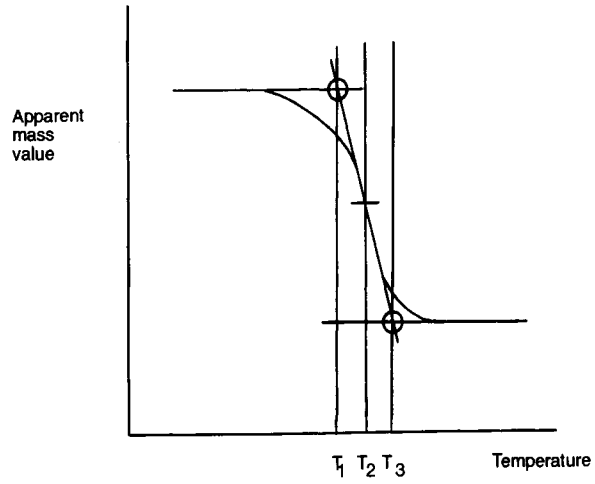

Figure 2.7 Curie point curve using the arrangement of Figure 2.4(c). For nickel, the reported values are: T_1 = 351.4 °C; T_2 = 352.8 °C; T_3 = 354.4 °C. T_2 is taken as the Curie point for calibration.

Table 2.1 Curie point calibration samples for TG

Sample	T_{Ci}/(°C)
Permanorm 3	259
Nickel	353
Mumetal	381
Permanorm 5	454
Trafoperm	750

If the magnetic material is placed in the sample holder and a magnet placed below the sample, as shown in Figure 2.4(c), the magnetic force on the sample will cause an apparent increase in mass. In a thermogravimetric run in nitrogen, the force will disappear fairly abruptly at the Curie point, as shown in Figure 2.7. The mid-temperature, or the peak of the DTG curve, is now used as a fixed point for calibration using the NIST materials listed in Table 2.1 [11,22].

Another method of calibration uses wires made from the high purity materials of very accurately known melting points such as those used in calibrating DTA [see Chapter 3]. These wires are used to attach a mass to the sample pan, which will detach immediately the wire melts [23].

A rough check on the calibration may be performed with known reactions, such as those given as examples later in this chapter, and

ensuring that the DTG peak temperatures match those obtained on the apparatus when it has been recently calibrated by a standard method.

2.4.6 *Atmosphere*

The need to surround the sample in an inert or a reactive atmosphere, and to control the evolution of gases from the sample, generally means that thermogravimetry is conducted in a flowing gas stream. Too high a flow rate can disturb the balance mechanism, while too low a flow rate will not remove product gases or supply reactant gas. Therefore, a flow rate of about 10–30 cm^3/min is often used. The flow of gas can also contribute to the transfer of heat and assist the transfer of products to any external gas analysis system [see Chapter 5].

If we wish to investigate a reaction that produces gas:

$$\begin{array}{lccccc} & A(s) & = & B(s) & + & C(g) \\ \text{e.g.} & CaCO_3 & = & CaO & + & CO_2 \end{array}$$

then we can conduct the experiment in a flowing inert atmosphere such as nitrogen, where the carbon dioxide will be swept away as soon as it is formed, or in an atmosphere of carbon dioxide, which will shift the position of equilibrium, according to Le Chatelier's Principle. If we consider a simple thermodynamic approach to the reaction, we have shown in Chapter 1 that the equilibrium constant for the reaction is given by:

$$K_p = \{p_{CO_2}\} \text{ equilibrium}$$

Since the reaction is *endothermic*, K_p increases as the temperature increases according to the van't Hoff equation:

$$\ln (K_p) = -\Delta H^{\ominus}/RT + \text{constant}$$

so the equilibrium pressure of CO_2 becomes greater.

At a low partial pressure of CO_2, decomposition will take place at a lower temperature than when the partial pressure is high.

If the sample is confined, then the atmosphere around it is made by the sample itself, that is, it is *self-generated*. This will cause similar effects to an externally imposed high pressure of product gases [24,25].

If we want the best contact between sample and surrounding gas, we must spread the sample thinly, or use a porous or gauze container, taking care that the sample holder is inert to all samples and gases [26,27].

2.5 Kinetics of reactions

The study of reactions can be divided into three parts:

1. The stages, intermediates and products of reaction.
2. The energetics of the reaction stages.
3. The reaction mechanism and reaction kinetics.

The first two parts may readily be studied by TG and DSC, and the third may also be investigated by thermal methods.

Consider a typical endothermic solid-state reaction:

$$\text{A (solid)} = \text{B (solid)} + \text{C (gas)}$$

As this reaction proceeds, gas and mass will be lost and heat absorbed. Several equations are used to model the process, but they may not be valid in all situations!

1. The extent of reaction ξ is a quantity having the dimension amount of substance and defined by:

$$n_B = n_{B,0} + \nu_B \cdot \xi$$

where n_B is the amount of substance B, $n_{B,0}$ is a chosen amount of B, e.g. at $t = 0$, and ν_B is the stoichiometric number of B, positive if B is a product, negative if B is a reactant [28].

For reactions in solution the progress of reaction is usually followed by the changes in concentration c_B of the species B with time, but for solid-state reactions this is hardly appropriate and it is more usual to follow the changes in the *fraction reacted*, α, with time.

The *rate of reaction* may now be written in terms of α:

$$\text{Rate} = d\alpha/dt$$

The rate of a reaction, even if measured at constant temperature, usually varies with time and with the value of α. It is therefore common to write:

$$\text{Rate} = d\alpha/dt = k_T, f(\alpha) \qquad (2.1)$$

where k_T is the rate constant at temperature T, and $f(\alpha)$ is a mathematical expression in α.

It would be nice if the same mathematical $f(\alpha)$ applied throughout the reaction, as is quite often the case for solution and radiochemical reactions, but it sometimes alters to a different $f'(\alpha)$ part-way through the reaction, due to the changes in mechanism, geometry or chemistry. It is easy to see why this should be so if we consider a thermogravimetric experiment where the different reaction stages overlap!

If a reaction is studied simultaneously by thermogravimetry and by a group-specific technique such as IR, the values of α may not be the same, since the IR-active species may not contribute to the greatest mass loss!

Relations used for the kinetics of solid-state reactions

Sestak and Berggren [29] summarised the many equations relating the rate of solid-state reactions to α. They may be written as a combined equation:

$$d\alpha/dt = k_T \cdot \alpha^m \cdot (1-\alpha)^n \cdot (-\ln(1-\alpha))^p$$

Table 2.2 Kinetic equations

Type	$f(\alpha)$ = Rate/k	$g(\alpha)=kt$
Order equations		
F1 First order	$(1-\alpha)$	$-\ln(1-\alpha)$
F2 Second order	$(1-\alpha)^2$	$1/(1-\alpha)$
Geometric		
R2 Contracting area	$2(1-\alpha)^{1/2}$	$1-(1-\alpha)^{1/2}$
R3 Contracting volume	$3(1-\alpha)^{2/3}$	$1-(1-\alpha)^{1/3}$
Acceleratory		
P1 Power law ($m>1$)	$m(\alpha)^{(m-1)/m}$	$\alpha^{1/m}$
Sigmoid curves		
An Avrami–Erofe'ev (n=2, 3 or 4)	$n(1-\alpha).$ $(-\ln(1-\alpha))^{(n-1)/n}$	$[-1n(1-\alpha)]^{1/n}$
B1 Prout–Tompkins	$\alpha(1-\alpha)$	$\ln(\alpha/(1-\alpha)) + c$
Diffusion		
D1 1-D diffusion	$1/(2\alpha)$	α^2
D2 2-D diffusion	$[-\ln(1-\alpha)]^{-1}$	$[(1-\alpha)\ln(1-\alpha)] + \alpha$
D3 3-D diffusion	$(3/2)(1-\alpha)^{2/3}$ $[1-(1-\alpha)^{1/3}]^{-1}$	$[1-(1-\alpha)^{1/3}]^2$
D4 Ginstling–Brounshtein	$(3/2[(1-\alpha)^{1/3}-1]^{-1}$	$[1-2\alpha/3]-(1-\alpha)^{2/3}$

It is sufficient to quote three examples and refer to the more comprehensive list in Table 2.2.

(a) One-dimensional diffusion-controlled reaction:

$$d\alpha/dt = k_T/2\alpha$$

(b) Two-dimensional growth of nuclei (Avrami equation):

$$d\alpha/dt = k_T(1-\alpha)\cdot(-\ln(1-\alpha))^{1/2}$$

(c) First-order reaction: random decay of active species:

$$d\alpha/dt = k_T(1-\alpha)$$

Upon integration, this last equation gives:

$$\ln(1/(1-\alpha)) = k_T \cdot t$$

or, for a general kinetic equation:

$$g(\alpha) = k_T \cdot t$$

The interpretation of the kinetic equation considers the way in which the reaction starts, by a process of nucleation, then how those nuclei grow and

what reaction or interface geometry is involved, and finally, how the reactants decay [30].

2. The rate constant, k, depends greatly on temperature and is thus sometimes written k_T. The equation used for many reactions is that of Arrhenius:

$$k_T = A \exp(-E/RT) \tag{2.2}$$

where A is the pre-exponential factor; E is the activation energy (J/mol) and R is the molar gas constant (8.314 J/(K mol)).

Several thermal analysis papers lament that different values of E have been found by different workers [31]. This may be due to a change in reaction mechanism during reaction, to a true variation in E or to differences caused by experimental procedure. The validity of the Arrhenius equation is very often assumed, and deviation attributed to changes in the mechanism [32].

3. The temperature in a non-isothermal experiment is ideally controlled, often to fit a linear programmed rise, β K/min:

$$T_t = T_0 + \beta \cdot t \tag{2.3}$$

This again is an ideal situation and for large sample masses, highly exothermic or endothermic reactions may cause changes in the real sample temperature. Urbanovici and Segal [33] suggest a modified equation:

$$T_t = T_0 + \beta \cdot t + s(t) \tag{2.3a}$$

where $s(t)$ is the difference between the sample temperature and the programmed temperature.

Therefore, it is as well when starting to study the kinetics of a reaction to beware of these pitfalls. A good guide to strategy for studying kinetics is given by Galwey [34] who advises the use of isothermal methods as well as rising temperature methods.

It may be as well to stress that the scheme recommends using complementary techniques, such as hot-stage and scanning electron microscopy, to confirm the mechanism of reaction.

Problems arise when equations (2.1)–(2.3) are combined and manipulated mathematically.

2.5.1 *Measurement of* α *and* dα/d*t*

For a thermogravimetric curve showing a single step, such as Figure 2.9, we may calculate α at a particular time, or temperature from the measured mass m_t and the initial and final masses, m_i and m_f.

$$\alpha = (m_i - m_t) / (m_i - m_f) = m_i / (m_i - m_f) - m_t / (m_i - m_f)$$

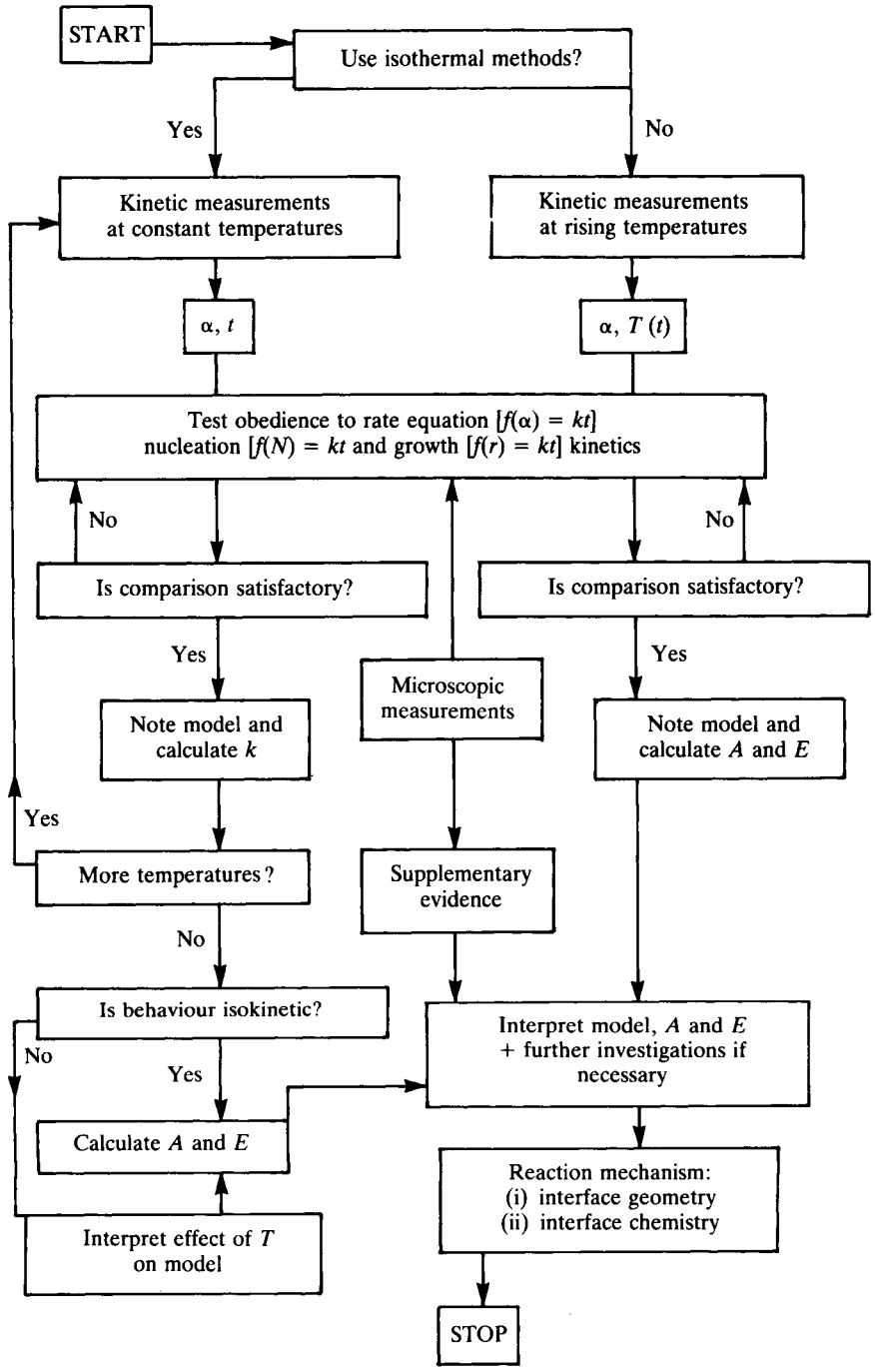

Figure 2.8 Schematic representation of the steps involved in the kinetic analysis of solid-state reactions. (From [34] with permission.)

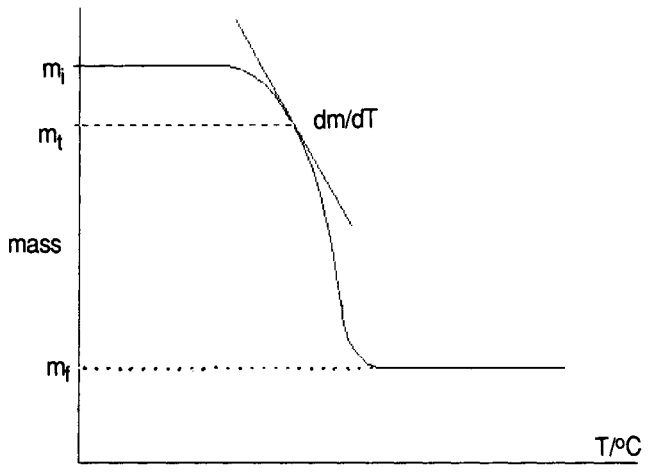

Figure 2.9 Schematic TG curve and the analysis for kinetics.

Differentiating this gives:

$$d\alpha/dt = -[dm_t/dt] / (m_i - m_f)$$

and we may therefore measure the rate of reaction from the slope of the mass–time curve. Since the DTG curve already measures dm_t/dt, this may be used to find $d\alpha/dt$ directly.

If we combine the linear heating equation (equation (2.3)), then:

$$dT/dt = \beta \tag{2.4}$$

and $d\alpha/dt = (d\alpha/dT) \cdot (dT/dt) = (d\alpha/dT) \cdot \beta$.

For a DSC curve, if the total area A represents the total reaction over the whole time or temperature interval and the fractional area α gives the partial reaction up to time t, then

$$\alpha = a/A$$

It has also been pointed out that the ordinate deflection y_t in DSC represents the rate of heat supply in J/s, so that we might also use it to find the rate, since $d\alpha/dt$ is proportional to y_t.

DIFFERENTIAL EQUATIONS

From equations (2.1) and (2.2):

$$d\alpha/dt = A \cdot \exp(-E/RT) \cdot f(\alpha)$$

Combining with equation (2.4)

$$d\alpha/dT = (A/\beta) \cdot \exp(-E/RT) \cdot f(\alpha) \tag{2.5}$$

Table 2.3

T(K)	$10^3k/T$	α	(1−α)	ln(1−α)	10^5.dα/dT	ln(dα/dT)
929	1.076	0.005	0.995	−0.005	6.25	−9.680
938	1.066	0.011	0.989	−0.011	8.86	−9.332
966	1.035	0.047	0.953	−0.048	19.28	−8.554
994	1.006	0.118	0.882	−0.125	37.51	−7.888
1013	0.987	0.194	0.806	−0.215	52.10	−7.560
1032	0.969	0.297	0.703	−0.277	68.77	−7.282
1050	0.944	0.432	0.568	−0.566	86.48	−7.053
1069	0.935	0.598	0.402	−0.911	102.6	−6.882
1078	0.928	0.691	0.309	−1.175	105.2	−6.857

Rearranging the variables and taking logarithms:

$$\ln(\mathrm{d}\alpha/\mathrm{d}T) - \ln(f(\alpha)) = \ln(A/\beta) - E/RT \qquad (2.6)$$

By plotting the left side of equation (2.6) against $1/T$, the activation energy can be obtained from the slope, and A from the intercept. In order to do this, we must have some idea of which $f(\alpha)$ we should use from Table 2.2!

Example For the decomposition of calcium carbonate, the kinetic equation could be one of many possible, for example:

1. Diffusion (D2: 2-D diffusion):

$$\mathrm{d}\alpha/\mathrm{d}t = k \cdot (-\ln(1-\alpha))^{-1}$$

2. Prout–Tomkins (B1: interacting nuclei):

$$\mathrm{d}\alpha/\mathrm{d}t = k \cdot \alpha \cdot (1-\alpha)$$

3. Mampel (R3: contracting sphere):

$$\mathrm{d}\alpha/\mathrm{d}t = 3k \cdot (1-\alpha)^{2/3}$$

We can test these by plotting the appropriate data according to equation (2.6). For example, the R3 plot would be of $\{\ln(\mathrm{d}\alpha/\mathrm{d}T) - (2/3)\cdot \ln(1-\alpha)\}$ against $1/T$.

For this experiment 10 mg of $CaCO_3$ powder was heated at 10 °C/min in a platinum crucible in flowing nitrogen. The TG plot was measured and selected data are given in Table 2.3 above.

It is very clear that the most appropriate kinetic equation is R3, the contracting sphere or Mampel equation. This agrees well with published data [35,36] although some references suggest an R2 law. The slope of the Mampel line is $-E/R$, and gives a value of E of about 190 kJ/mol. This is a little high, but comparable to some published data. Reading has pointed out [31] that the range of values quoted for the activation energy of this reaction is very large indeed! The pre-exponential factor A is about 10^7 s^{-1}.

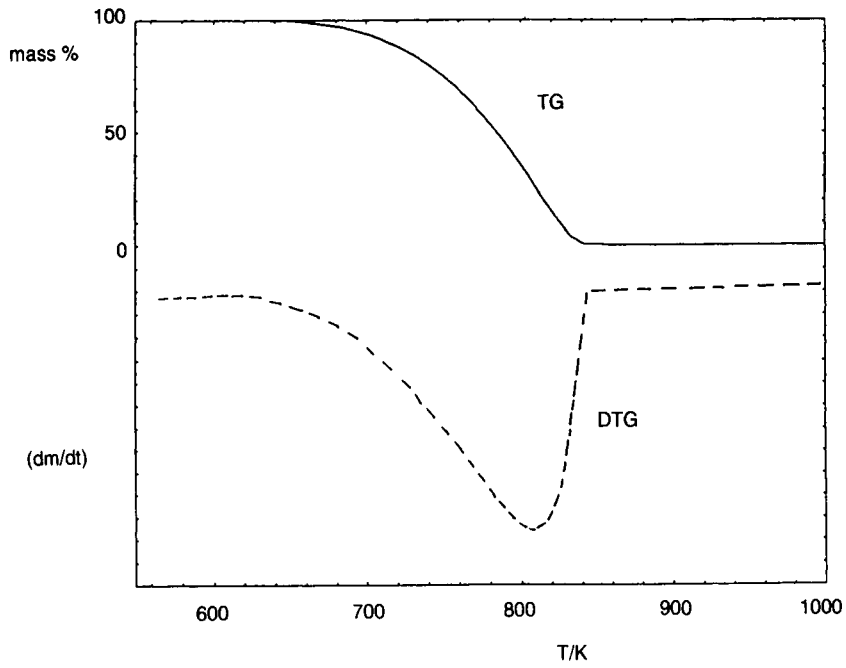

Figure 2.10 TG and DTG curves for 10 mg of $CaCO_3$ powder heated at 10 K/min in flowing nitrogen (30 cm^3/min).

REDUCED TIME PLOTS

In order to check the validity of the kinetic equation and which $f(\alpha)$ should be used, it is good practice to plot all results onto the same graph [4,37]. For isothermal cases, plotting the value of α against $(t/t_{0.5})$ often gives a single trace of characteristic shape, as shown in Figure 2.12. If the value of $f(\alpha)$ is evaluated from the equations of Table 2.2, the fit of the observed data can identify the kinetic rate equation. For example, for a first-order (F1) mechanism,

$$\alpha = 1 - \exp(-0.693(t/t_{0.5}))$$

Similar reduced plots have been suggested for non-isothermal results [38] and for constant rate results [39].

INTEGRAL METHODS

If we attempt to use the integrated rate equations represented by the functions $g(\alpha)$ in Table 2.2, the integration of equation (2.5) is required.

$$g(\alpha) = \int d\alpha/f(\alpha) = (A/\beta) \cdot \int (\exp(-E/RT))\, dT \qquad (2.7)$$

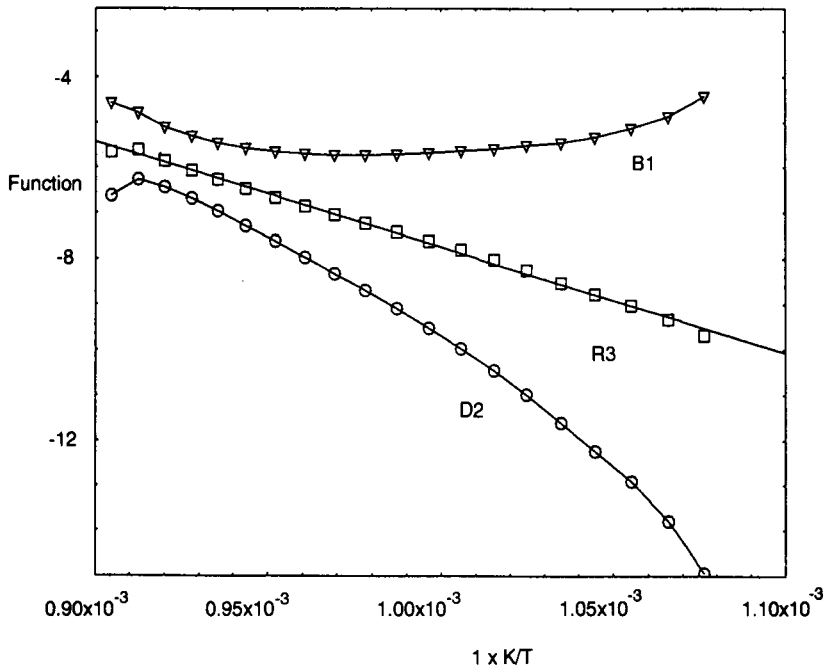

Figure 2.11 Plots of $\ln(d\alpha/dT) - \ln(f(\alpha))$ against $1/T$ for diffusion (D2), Prout-Tomkins (B1) and Mampel (R3) kinetics applied to calcium carbonate decomposition.

This involves the difficult integration of the right-hand side temperature integral. If we assume that $\alpha = 0$ until the reaction starts at T_i, we may change the limits of integration and integrate from 0 to T:

$$\int (\exp(-E/RT))\, dT = (E/R) \cdot \int [(\exp(-x))/x^2]\, dx = (E/R) \cdot p(x)$$

where $x = E/RT$ and $p(x) = [(\exp(-x))/x^2]$.

Approximations to determine $p(x)$ have been proposed, one of the best of which is

$$p(x) \approx \exp(-x)/[x(x+2)]$$

Values of the function $p(x)$ may be calculated by computer and have been tabulated. Various approximations have been suggested for the temperature integral, for example: Doyle [40];

$$\log_{10} p(x) \approx -2.315 - 0.4567x \quad (\text{for } x > 20) \tag{2.8}$$

Coats and Redfern [41]:

$$g(\alpha) = (ART^2/\beta E)\,[1-(2RT/E)] \cdot \exp(-E/RT)$$

Brown [42] gives an excellent discussion of the mathematics used and the treatment of kinetic results. Ozawa [43] and Flynn and Wall [44] have

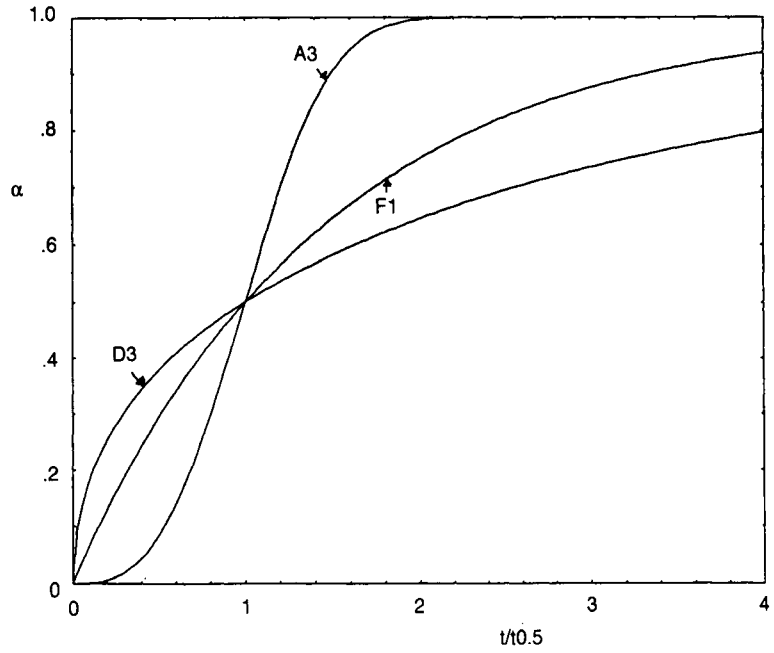

Figure 2.12 Reduced time plots for Avrami (A3), first-order (F1) and 3-D diffusion (D3) kinetics.

shown that if different heating rates, β, are used, the temperature T_α for a given conversion α may be shown, by combining equations (2.7) and (2.8), to be

$$\log_{10} \beta = -2.315 + \log_{10} (AE/R) - \log_{10} g(\alpha) - 0.4567(E/RT_\alpha) \quad (2.9)$$

Plotting log α against $1/T_\alpha$ generally gives good straight lines of slope $-0.4567\ (E/R)$. The pre-exponential factor, A, is also obtained by equation (2.10)

$$A = \beta \cdot (E/RT^2) \cdot \exp(E/RT) \quad (2.10)$$

A revision of the value of E determined by this method uses a correction value of $D = -\ \mathrm{d} \ln(p(x))/\mathrm{d}x$, which is tabulated in ASTM E 698, or may be evaluated by computer.

Example Since the kinetics of decomposition of polymeric materials is a very important study and relates to their stability and performance, the thermal decomposition of poly(tetrafluoroethylene), PTFE, was studied by TG [45] using samples of about 10 mg, and flowing air at 30 cm^3/min.

Rate, β(K/min)	*T*(K) (2%)	*T*(K) (10%)
2.5	775	798
5.0	781	805
10	791	818
20	802	829

The slopes of the plots are -1.80×10^4 and -1.67×10^4 K, so that

$E \approx -(1/0.4567) \times R \times \text{slope} \approx -2.19 \times R \times \text{slope}$
$E \approx 328$ kJ/mol and 304 kJ/mol, giving an average
$E = 316$ kJ/mol

The values are refined by calculating $x = E/RT$ for a temperature in the middle of the range, say 790–810 K, and looking up D in tables. For an average value:

$x = 47.5$, so that $D = 1.042$
$E \approx -2.303 \times R \times \text{slope}/D = 319$ kJ/mol

This procedure may be repeated until a constant value of E is obtained. Using the mid-point value of 10 K/min

$A = 10\,(319\,000/(8.314 \times 800^2)) \cdot \exp(319\,000/(8.314 \times 800))$
$A = 4.05 \times 10^{20}\ \text{min}^{-1}$

It may be noted that, for reactions having several stages, the value of E may change as a function of the degree of conversion, and this has been illustrated with the pyrolysis of poly(1,4-phenylene-di(methoxyphenyl)-vinylene) in argon [46] where the reaction shows three stages with activation energies of 200, 263 and 258 kJ/mol.

CONSTANT RATE METHODS

If we consider that the rate of reaction ($d\alpha/dt$) is controlled by the value of the temperature, the fraction reacted and the nature of the atmosphere, then control of these parameters could be used to control the rate directly.

Rouquerol [47] proposed that 'a quantity directly related to the decomposition rate is kept constant'. This quantity may be the evolved gas flow, the thermal flow or the DTG signal. This is the technique of constant rate thermal analysis (CRTA). The quasi-isothermal, quasi-isobaric techniques of the Pauliks [48] controlled their system in such a way as to keep the rate of mass loss constant, and to confine the reaction gases so that they were lost at constant atmospheric pressure.

Reading [39] has described the 'rate jump' technique, where the temperature and pressure are controlled such that, at a temperature T_1, the rate of mass loss is constant at $(d\alpha/dt)_1$, and when it is rapidly raised to a new temperature T_2, the new constant rate is $(d\alpha/dt)_2$. For a small interval, the value of $\ln[f(\alpha)]$ changes little during the jump, so that:

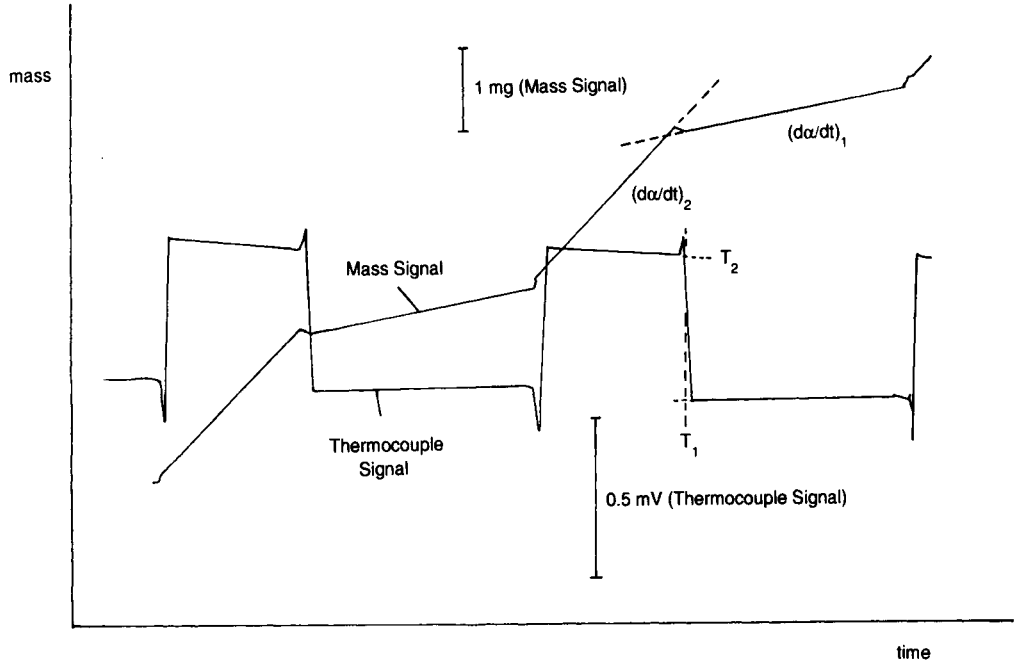

Figure 2.13 Typical results for rate jump constant rate thermal analysis [39].

$$E = \frac{-R \ln[(d\alpha/dt)_1/(d\alpha/dt)_2]}{(T_2 - T_1)/(T_1 \cdot T_2)}$$

For calcium carbonate, a value of E= 193 kJ/mol was reported.

2.6 Applications of thermogravimetry

A selection of examples is given below, but the range of applications is very large indeed. Readers are advised to study the specialist texts on thermogravimetry for further particulars.

Note! It must be remembered that TG will ONLY detect changes where the mass of the sample changes, by reaction, or vaporisation, or because a physical property changes its interaction with an imposed external force, e.g. the magnetic permeability in an imposed magnetic field.

2.6.1 *Thermogravimetric curves*

DECOMPOSITION OF MAGNESIUM HYDROXIDE ($Mg(OH)_2$)

This is found as a natural mineral, brucite; it is used in gravimetric analysis and as a fire-retardant additive in polyamides, polyolefins and polyesters.

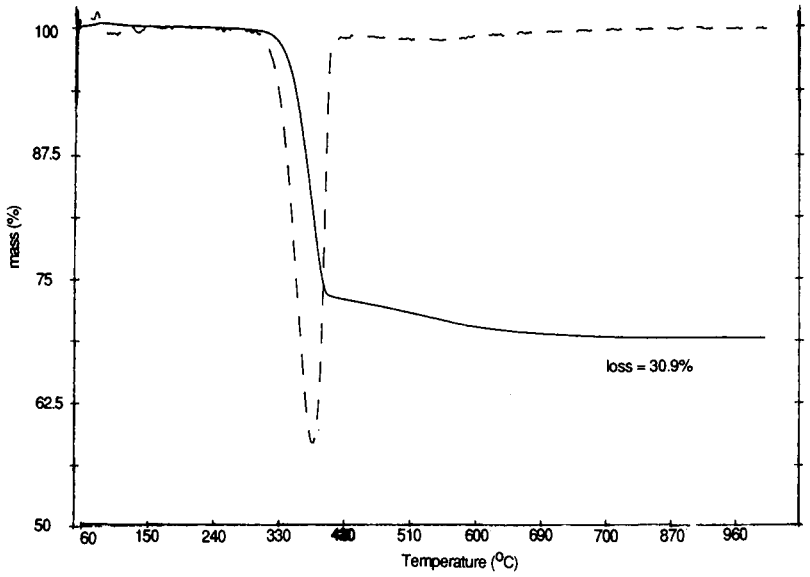

Figure 2.14 TG and DTG curves for magnesium hydroxide, 7.04 mg, heated in a Pt crucible at 10 K/min, nitrogen.

The thermogravimetric trace of a commercial sample given in Figure 2.14 shows a single mass loss over a fairly broad temperature range. The sample is stable up to about 200 °C, and then loses about 27% of its mass rapidly by 450 °C; a much slower loss then occurs up to 800 °C with a total mass loss of 30.9%.

The chemical equation for the reaction is:

$$Mg(OH)_2(s) = MgO(s) + H_2O(g)$$

and the water evolved can be detected by chemical, physical or spectroscopic techniques (see Chapter 5). The stoichiometry of the above reaction suggests that the calculated loss should be

$$\% \text{ Loss} = 100 \times M(H_2O)/\, M(Mg(OH)_2) = 100 \times 18.0/58.3$$
$$= 30.87\%$$

Thus we see a very good agreement between theory and experiment in this case. The reason for the two stages shown on the TG and DTG curves is less obvious. It has been attributed to the rapid reaction to decompose all the hydroxide and to lose the majority of the water vapour, followed by the gradual slow diffusion of water vapour adsorbed on, or trapped within, the oxide [49]. Another alternative is the presence of a small amount of carbonate impurity [50].

Samples prepared by different reactions, or stored under different

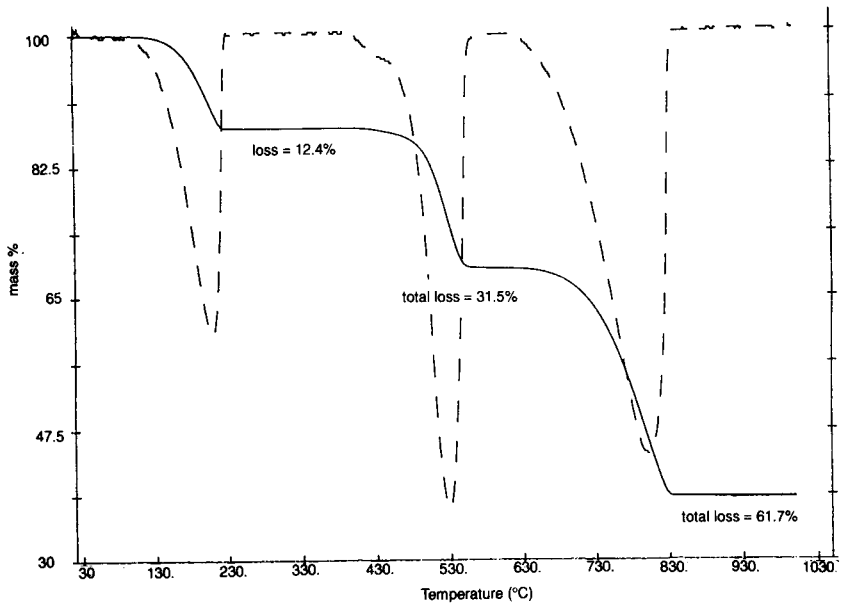

Figure 2.15 TG and DTG curves for calcium oxalate monohydrate, 12.85 mg, Pt crucible, 20 K/min, nitrogen.

conditions, or subjected to different packing [51] have all been shown to give different TG curves, although the quantitative nature of the change is unaffected.

The endothermic nature of the dehydration reaction is one reason for the use of magnesium hydroxide as a fire retardant, and it is found that incorporating it into a polymer changes the decomposition of *both* the polymer and the hydroxide.

CALCIUM OXALATE MONOHYDRATE ($CaC_2O_4 \cdot H_2O$)

The oxalate hydrates of the alkaline earth metals, calcium, strontium and barium, are all insoluble and have been used in gravimetric analysis. For example, a calcium salt in a solution made acidic with ethanoic acid, when treated with an excess of sodium oxalate solution, precipitates calcium oxalate monohydrate quantitatively [52]. The precipitate is washed with ethanol, and may then be analysed as one of three compounds:

- as $CaC_2O_4 \cdot H_2O$, by drying at 100–115 °C for 1–2 hours;
- as $CaCO_3$ by heating to 475–525 °C in a furnace;
- as CaO by igniting at 1200 °C.

When we heat this compound on a thermobalance, we obtain the curves shown in Figure 2.15. A single run in air at 10 °C/min up to 1000 °C shows three distinct changes:

1. Between room temperature and about 250 °C there is a loss of about 12% to give a stable product.
2. Between 300 and 500 °C a loss of some 19% occurs to give a second stable product.
3. Above 600 °C there is a final loss of about 30% to give a final product stable to the highest temperature used.

Can we suggest a set of reactions to explain these losses?

1. Since the first loss starts around 100 °C, we might consider loss of water vapour:

   $CaC_2O_4 \cdot H_2O(s) = CaC_2O_4(s) + H_2O(v)$
   Calculated % loss $= 100 \times 18.0/146.1 = 12.3\%$

   This loss corresponds with what is found, so this reaction is *possible*.
2. Previous analytical methods produced calcium carbonate by heating to about 500 °C, so let's consider that:

   $CaC_2O_4(s) = CaCO_3(s) + CO(g)$
   Calculated % loss $= 100 \times 28.0/146.1 = 19.2\%$

   This, too seems a likely reaction!
3. The decomposition of calcium carbonate is a well-established reaction:

   $CaCO_3(s) = CaO(s) + CO_2(g)$
   Calculated % loss $= 100 \times 44.0/146.1 = 30.1\%$

Words of caution! Despite the excellent agreement of the calculated and experimental values, it is *most unwise* to deduce reaction schemes from this evidence alone! The products, both gaseous and solid, should be characterised by other analytical methods, such as X-ray diffraction for solids and chemical tests for gases.

In the particular case of calcium oxalate described above, these tests have been made, and the stages of decomposition confirmed. The presence of calcium oxalate hydrate in kidney stones [53] extends the use of this analysis to biological fields.

If the conditions of analysis are changed, the temperature ranges of the events may alter, and the shape of the curve change, but the stable products will still be obtained. We shall see later that this analysis may be adapted to determine calcium, strontium and barium simultaneously [52].

COPPER SULPHATE PENTAHYDRATE ($CuSO_4 \cdot 5H_2O$)

Blue hydrated copper sulphate is a very well known material and has been used to demonstrate many thermal techniques. In this example, we shall

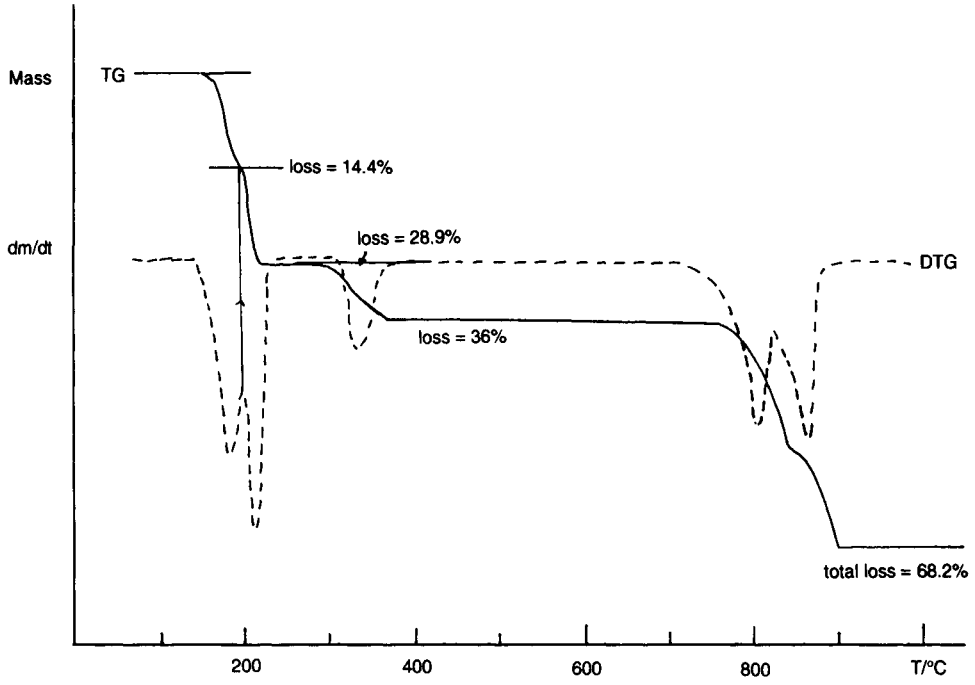

Figure 2.16 TG and DTG curves for copper sulphate pentahydrate, 10.61 mg, alumina crucible, 10 K/min, air.

show how the DTG curve may be used to help obtain quantitative data. Depending on the conditions, the stages of the reactions may be resolved to different extents. If a very fast heating rate and large sample is used, the stages tend to 'blur' together. Conversely, at slow heating rates, or where the rate of reaction is controlled, the stages are well resolved.

The sample heated for Figure 2.16 shows a mass loss starting below 100 °C, closely followed by a further loss up to 160 °C. The DTG curve shows a minimum from which the mass losses for the two overlapping stages may be calculated, using the construction shown.

By checking the mass losses, you can confirm the following *possible* set of decomposition reactions. (RAM are: Cu = 63.55; S = 32.06; O = 16.00; H = 1.00.)

1. $CuSO_4 \cdot 5H_2O(s) = CuSO_4 \cdot 3H_2O(s) + 2H_2O(v)$
2. $CuSO_4 \cdot 3H_2O(s) = CuSO_4 \cdot H_2O(s) + 2H_2O(v)$
3. $CuSO_4 \cdot H_2O(s) = CuSO_4(s) + H_2O(v)$
4. $CuSO_4(s) = CuO(s) + SO_2(g) + \frac{1}{2}O_2(g)$

What does the DTG curve suggest about the reaction above 700 °C? One explanation given is that a basic sulphate, $CuO \cdot CuSO_4$, is formed.

DEGRADATION OF POLYMERS

The effects of heat on polymeric materials varies greatly with the nature of the polymer, ranging from natural polymers like cellulose, which start to decompose below 100 °C, to polyimides which are stable up to 400 °C. The presence of additives and the atmosphere used also affect the changes greatly.

When heated in an inert atmosphere, polymeric materials react by two general routes, often related to their mode of polymerisation and the heat of polymerisation. They may either *depolymerise* or *carbonise* [4,54].

Polymers such as poly(methyl methacrylate) (PMMA) and polystyrene (PS) may depolymerise or 'unzip' back to the monomer. Such polymers generally have a low ΔH of polymerisation. Random scission of poly-(alkenes) like poly(ethylene) (PE) will produce unsaturated hydrocarbons from chain fragments of varying lengths like butenes, hexenes and dienes. The kinetics of this random process is approximately first order, and the temperatures of degradation are much affected by the substitution. Thus, with fluorine substitution, poly(tetrafluoroethylene) (PTFE) decomposes at a much higher temperature than PE, and with methyl substitution, poly(propylene) (PP) at a lower temperature than PE, as shown in Figure 2.17.

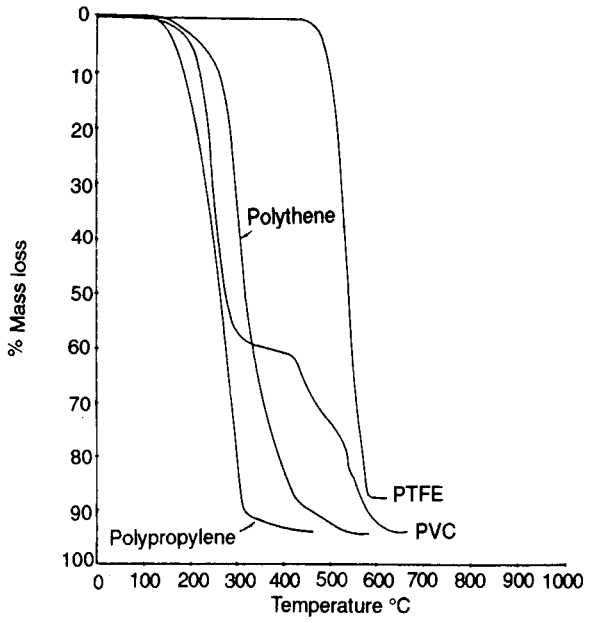

Figure 2.17 TG curves for polymer samples in air. Samples all about 1 mg, heated at 50 K/min.

Poly(vinyl chloride) (PVC) and poly(acrylonitrile) (PAN) may eliminate small molecules initially and form unsaturated links and cross-links before finally degrading by complex reactions to a char, which will oxidise in air.

$$R\text{—}(CH_2\text{—}CH\cdot Cl\text{—})_n\text{—}R' \rightarrow R\text{—}(CH{=}CH)\text{—}R' + HCl \rightarrow \text{etc.}$$

This stage is shown in Figure 2.17 as a loss of about 60%.

Polymers containing polar groups, such as polyamides (e.g. nylon 66), may absorb moisture which is usually lost below 100 °C, sometimes in stages if the moisture is in different environments.

Cellulose polymers, polyester resins and phenol–formaldehyde polymers have extremely complex decomposition schemes, eliminating small molecules, often flammable or toxic, and eventually leaving a charred mass. If a polymer melts during degradation, a *coke* is formed.

In an oxidising atmosphere, these reactions are further complicated, both by the oxidative attack on the polymer, forming peroxides, and also by the oxidation of the products and char.

Flame-retardant additives in polymers may be studied since their mode of action may alter the nature of the reactions and the amounts of products.

In Figure 2.17, several polymers are compared and their relative stabilities may be assessed. The initial temperature of degradation may not be comparable to the maximum continuous use temperature, since thermoplastics may melt, and this would not show on TG, and other polymers degrade slowly over a long period, even at low temperatures.

A cautionary note on the use of thermal methods of stability assessment was sounded by Still [56], whose review considers instrumental and procedural problems and the effects of polymer structures. Cullis and Hirschler [57] consider thermal methods as applied to the combustion of polymers, and Turi [58] provides a comprehensive review of polymer applications of thermal methods.

2.6.2 *Analysis of mixtures*

When we wish to analyse an unknown mixture of chemical substances in a real sample, several options are open to us. We may use the wide range of separation techniques such as chromatography to isolate each component of the mixture, which may then be identified and measured separately, or we may use a solution technique such as inductively coupled plasma spectrometry which can determine all the elements present simultaneously. However, neither of the above methods is suitable to the entire range of solids from minerals to polymers, and both require a change in the original material before analysis.

Thermogravimetry shows the differences between the behaviours of

substances on heating, and if those behaviours are sufficiently different on the temperature scale, the individual reactions of substances may be identified and measured. Three examples will be given from a wide range.

MIXTURES OF ALKALINE EARTH OXALATES

We have already seen how the decomposition of calcium oxalate hydrate may be followed by TG. The oxalates of magnesium, strontium and barium are also precipitated under similar conditions, but decompose in rather different ways [52].

Magnesium oxalate dihydrate breaks down in only *two* stages: firstly, to the anhydrous oxalate by about 250 °C, and then directly to the oxide by 500 °C.

Strontium oxalate monohydrate and barium oxalate hemihydrate lose water by 250 °C and the anhydrous oxalates decompose to the carbonates by 500 °C. The strontium carbonate decomposes between about 850 and 1100 °C while the barium carbonate is stable until even higher temperatures. An illustration of the decomposition of the mixture of calcium, strontium and barium oxalate hydrates is shown in Figure 2.18 and the percentages of each may be found from the TG trace.

A comparison of the thermodynamics of decomposition of metal oxides or metal carbonates (Figure 2.19) may be done by the construction of Ellingham diagrams [59]. These involve the plotting of $\Delta G^{\ominus}$ against T for the reaction of importance, for example:

$$M_mCO_3(s) = M_mO(s) + CO_2(g)$$

For this reaction ΔG and ΔH are generally positive at 298 K (25 °C) and ΔS is very positive since gaseous carbon dioxide is produced. For calcium carbonate, for example, at 298 K:

$$\Delta G^{\ominus} = 130.1 \text{ kJ/mol};$$
$$\Delta H^{\ominus} = 177.9 \text{ kJ/mol; and } \Delta S^{\ominus} = 160.4 \text{ J/(K mol)}$$

The slope of the Ellingham plot is:

$$(\partial \Delta G^{\ominus}/\partial T)_p = -\Delta S^{\ominus}$$

and is negative since $\Delta S^{\ominus}$ is very positive. This means that $\Delta G^{\ominus}$ becomes less positive and finally passes through zero to become negative as the temperature increases. When $\Delta G^{\ominus}$ is zero, the equilibrium pressure of carbon dioxide is 1 atmosphere and the carbonate will decompose. We may call this a 'decomposition temperature T_d', although the material may decompose at other temperatures under other conditions.

It has been shown that the value of T_d depends upon the cation radius, r, and a good correlation is found plotting $\Delta H^{\ominus}$ vs $(r^{1/2}/z^*)$ where z^* is the effective nuclear charge.

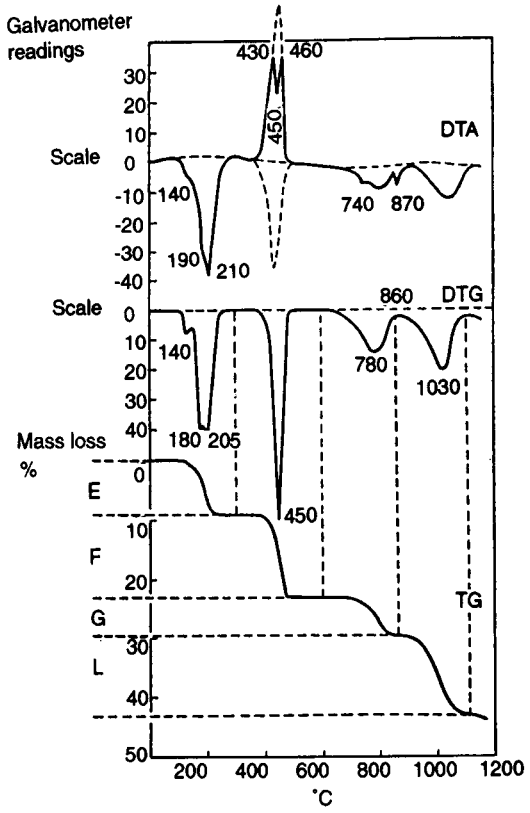

Figure 2.18 Derivatograph trace for a mixture of calcium, strontium and barium oxalate hydrates, about 0.3 g, heated at 10 K/min [52]. The stages are as follows: loss of water of crystallisation (E); loss of CO from decomposition of the oxalates (F) and loss of CO_2 from calcium carbonate (G) and from strontium carbonate (L).

Mixtures of carbonates and mixtures of nitrates may be analysed quantitatively by TG and examples are given at the end of this chapter and in Chapter 6. Dollimore *et al.* [60] have shown the applicability of the thermodynamic treatment to more complex systems.

POLYMER BLENDS

Since the decomposition profiles of polymers are characteristic, some polymer blends [61,62,63] may be analysed by TG. Figure 2.20 shows the TG of a ethylene–vinyl acetate (EVA) copolymer heated at 20 K/min in nitrogen. The first loss may be shown to be ethanoic acid (acetic acid) from the vinyl acetate, while the second shows the decomposition of the residual material.

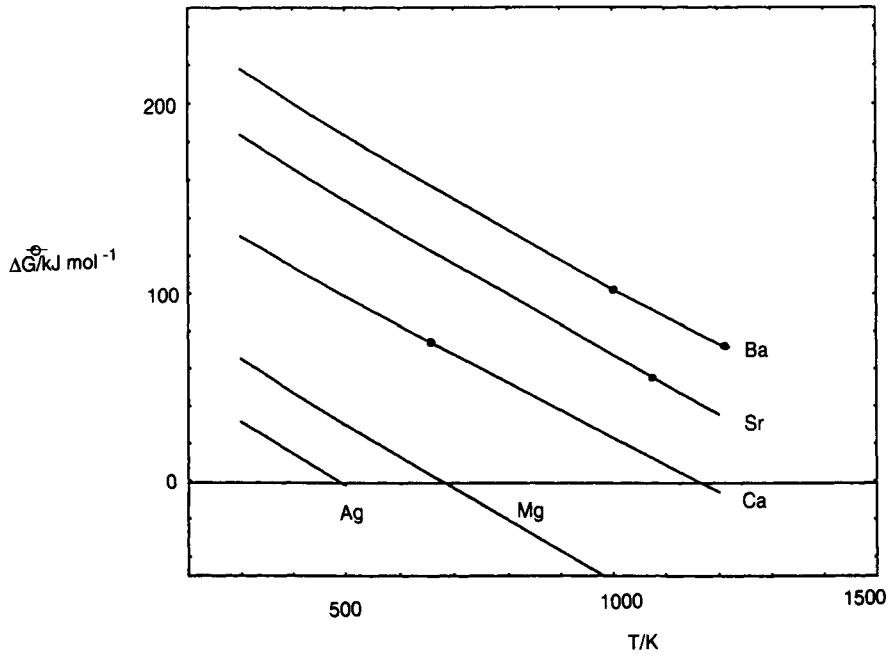

Figure 2.19 Ellingham diagram for the decomposition of carbonates: $M_mCO_3 = M_mO + CO_2$. Full points represent phase transitions [35].

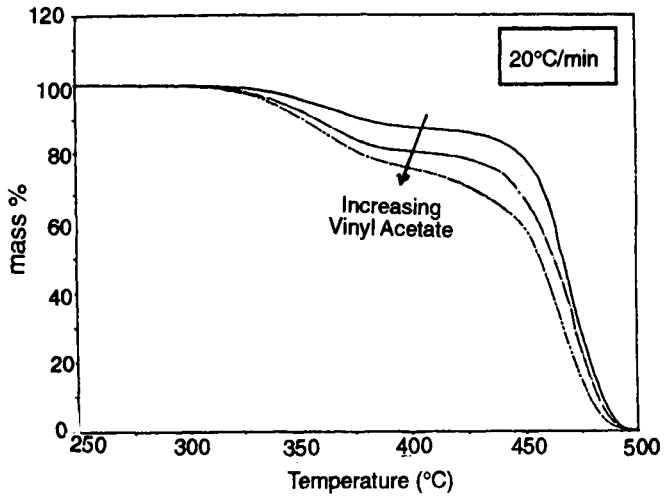

Figure 2.20 TG curves for ethylene–vinyl acetate blends. Samples of about 10 mg run in nitrogen at 20 K/min. (Courtesy TA Instruments Ltd.)

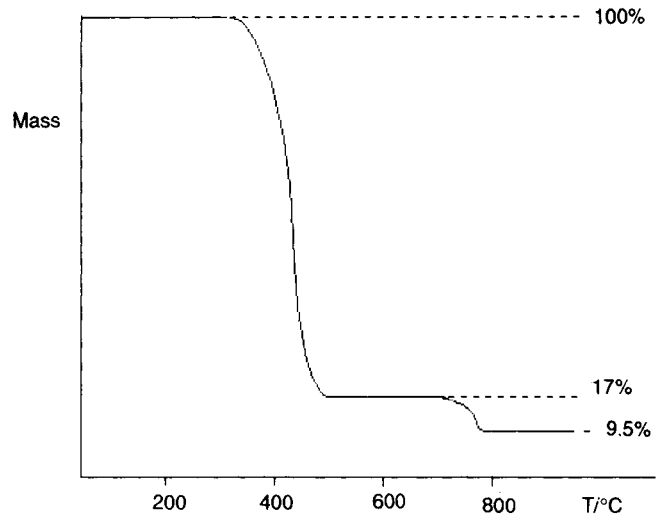

Figure 2.21 TG curve for polyolefin polymer with $CaCO_3$ filler. Sample of 10.5 mg heated at 10 K/min in nitrogen. Residue at 500 °C gives the filler content (17%) and the temperature and percentage mass loss for decomposition (about 700 °C and 44% loss) suggest $CaCO_3$.

Polymers containing additives, especially fillers like calcium carbonate and fire-retardants such as aluminium hydroxide, are often studied by TG. The decomposition stages may be altered, but the residue at high temperature is characteristic of the filler. For example, calcium carbonate shows the normal decomposition to calcium oxide around 800 °C and aluminium hydroxide leaves a stable residue of Al_2O_3. Figure 2.21 shows one example of this.

The quantitative analysis of filled polymers and rubbers may also involve oxidation. Figure 2.22 shows a rubber material filled with carbon. The stages of decomposition are well defined, and start in nitrogen atmosphere with the loss of a volatile oil component below 200 °C followed by the degradation of the main polymer components. The residue at 600 °C is stable in nitrogen, but on switching to air the carbon-black filler is oxidised away, leaving the small ash content. We thus have four analyses performed in one TG run. It should be noted that the decomposition products of the polymer are often very flammable and care must be taken to remove them before introducing any air!

SOILS

The composition of soils [2,64,65] is complex, and varies with the geological and biological nature of the area, the level from which the soil

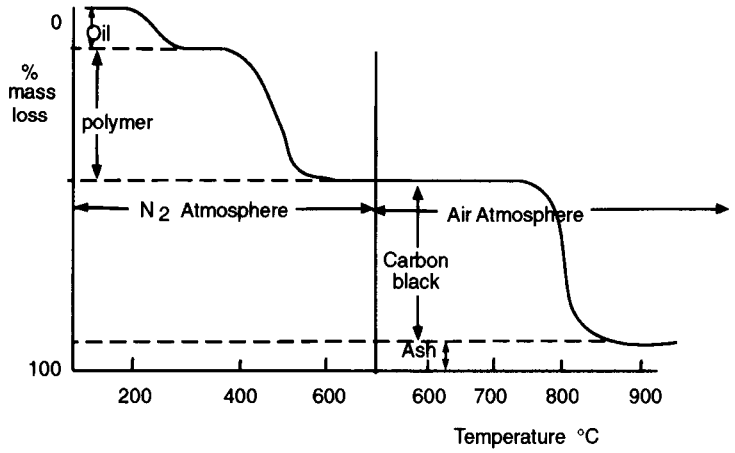

Figure 2.22 TG curve for carbon-black filled rubber. (Courtesy PL-Thermal Sciences.)

was collected and the human and biological interaction that has taken place. After soil samples have been collected, they should be stored under reproducible conditions, e.g. constant relative humidity for about 1 week. There are generally three stages of soil decomposition on heating:

1. Loss of hygroscopic moisture and of simple volatiles produced from organic compounds between room temperature and 150 °C.
2. Ignition of organic matter starts at about 250 °C and is complete by 550 °C. The organic matter may be determined by the mass loss between these two temperatures, provided no other reactions interfere. The largest interference comes from clay minerals, but provided the clay content is less than about 40%, the loss to 500 °C is a very good guide to the organic matter. An alternative is to remove the organics by wet oxidation using hydrogen peroxide, and then run the residue.
3. Hydrated minerals such as aluminium and iron oxides, and micas and gypsum may complicate matters, but high-temperature decompositions can show the content of minerals such as carbonates.

COALS

The analysis of coals [66,67] for moisture, total volatiles, fixed carbon and ash content is referred to as a 'proximate analysis'. Thermogravimetry, especially when computer controlled, has great advantages over traditional methods for proximate analysis. Figure 2.23 shows the TG curve of a typical coal, and the alterations in heating rate and in atmosphere required

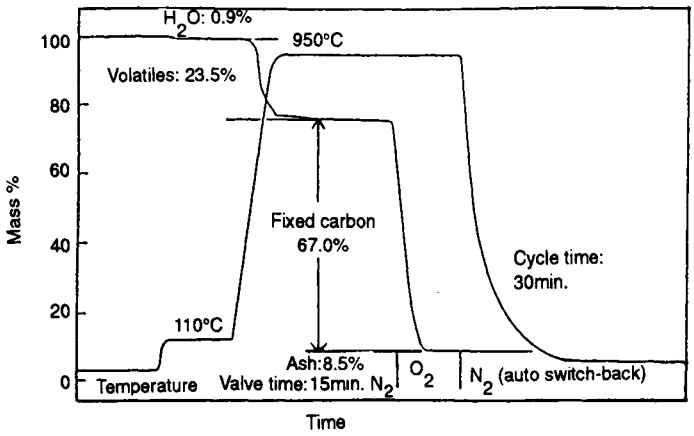

Figure 2.23 Proximate analysis of coal using microcomputer-controlled thermogravimetry [67].

to obtain results in the optimum time. It is most important that each stage is completed before starting the next, especially when switching to an oxidising atmosphere, where any remaining flammable gases may combust explosively at high temperature in oxygen or air.

2.6.3 *Oxidation studies*

Besides the oxidation of organics and of carbon, studies have been made of the oxidation of metals and alloys [68–70] and of compounds [71] using thermogravimetry.

In this instance it is often useful to run the sample *isothermally*. Figure 2.24 shows the oxidation of metallic copper in air at 800 °C. The curve is unusual in showing a weight *gain*! Where this is observed in other traces it often indicates metal oxidation. The oxidation of copper forms Cu_2O first. The shape of the curve may be fitted to the parabolic law governing the kinetics of metal oxidation and may show a broken parabola if the oxide surface cracks [72].

2.6.4 *Reduction studies*

The preparation of catalysts often involves a reduction step. The use of TG apparatus and of special *temperature programmed reduction* (TPR) apparatus, which measures continuously the consumption of hydrogen during the reduction process, has given much useful data on catalyst preparation and allowed the detection of overlapping reactions and the study of kinetics [73,74].

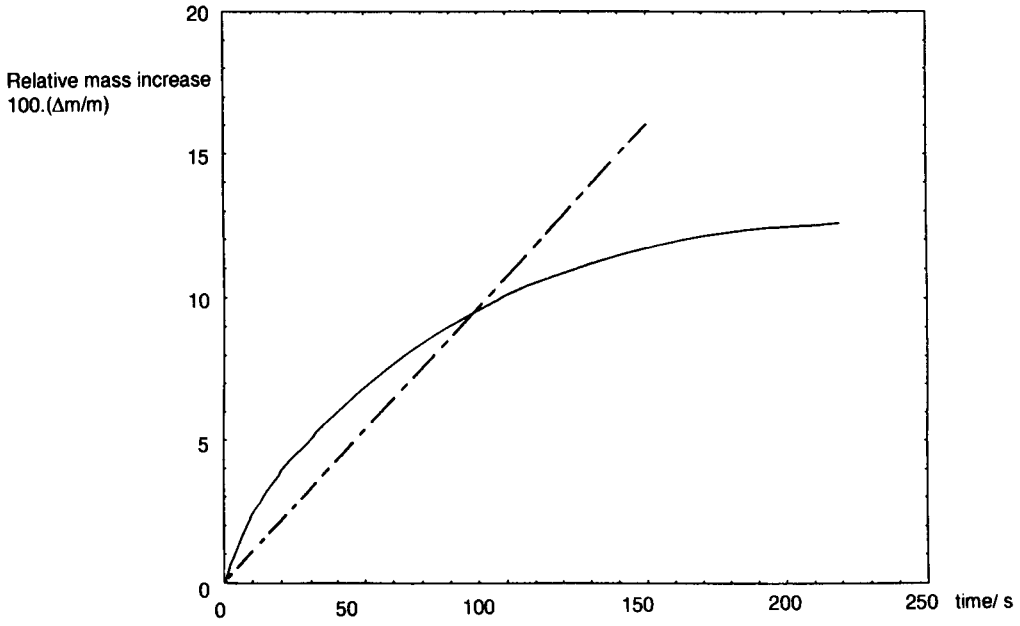

Figure 2.24 Isothermal TG oxidation curve for copper metal. Sample of copper turnings, 20 mg, heated at 800 °C in air. Relative mass increase (full line) and $(\Delta m/m)^2$ (dashed line) for parabolic rate law.

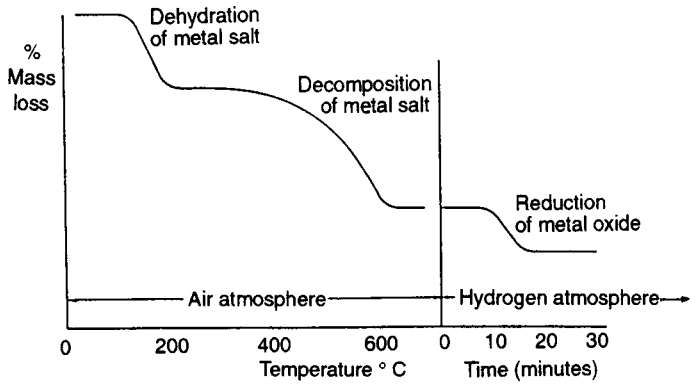

Figure 2.25 TG curve for the decomposition of a metal salt in air. When the decomposition to the oxide is complete at just above 600 °C, the temperature is held constant and the atmosphere changed to H_2, causing reduction to the metal [75].

In a similar way to that described in section 5 above, the atmosphere may be changed during the run so that the product is reduced. This is shown in Figure 2.25.

2.7 Controlled rate thermogravimetry and Hi-Res™ TGA

In the usual TG experiments, the analyst sets a *constant heating rate* and measures the temperature and mass as dependent variables, as a function of time. If several reactions occur, it is important that we try to resolve them. Of course, the atmosphere gases, the instrumental conditions and the nature of the sample, plus the kinetics of the reactions occurring, will affect the extent to which the reactions may overlap. Very small samples will help, producing less interference between products and reactants, and very low heating rates will help by allowing one reaction to finish before the next begins. However, these conditions cause problems, either of sensitivity, or of a very long time needed for the experiment, perhaps several hours if isothermal or at a very slow heating rate.

Another method of improving the resolution is to control the *rate of reaction*. This may be done by sensing the rate of mass loss [48] or by sensing the evolution of a particular product gas [47] and using one of these parameters to control the rate of heating. Generally these methods have led to longer experimental times than for a conventional TG run.

Commercial equipment is now available [76] which achieves the benefit of higher resolution of thermal events without sacrificially long experimental time. With microprocessor control, when no mass loss is occurring, it is possible to have a high heating rate (for example, 50 K/min), but when a loss is detected the heating rate is reduced towards zero, and kept low until the mass again becomes nearly constant. One analogy is with a video recorder. If nothing of interest is happening, we can 'fast forward' the videotape. When an important event shows up, we can slow down or even 'pause' the tape.

For rapid sensing and control, it is necessary to have a thermocouple close to the sample, plus a directed purge gas flow for rapid removal of product gases and interchange with the sample, plus a thermobalance system of high sensitivity to detect small mass changes and respond rapidly. The commercial Hi-Res™ TGA system allows the operator to programme in the resolution required, from a very high resolution where the experimental time may be long, to a 'standard' experiment with a run giving much higher resolution than a normal TG, but a comparable run time.

Applications of Hi-Res™ TGA have been reported for various materials, from improved resolution for the dehydration and decomposition of copper sulphate, to the analysis of fuel transport additives. Three examples showing the improvements that may be obtained will be given.

2.7.1 *Polymer blends*

We have noted above the possibility of analysing ethylene–vinyl acetate (EVA) copolymers by TG (see Figure 2.20). Although the steps are fairly well resolved with conventional TG, Hi-Res™ TGA improves this dramatically and gives better quantitative accuracy.

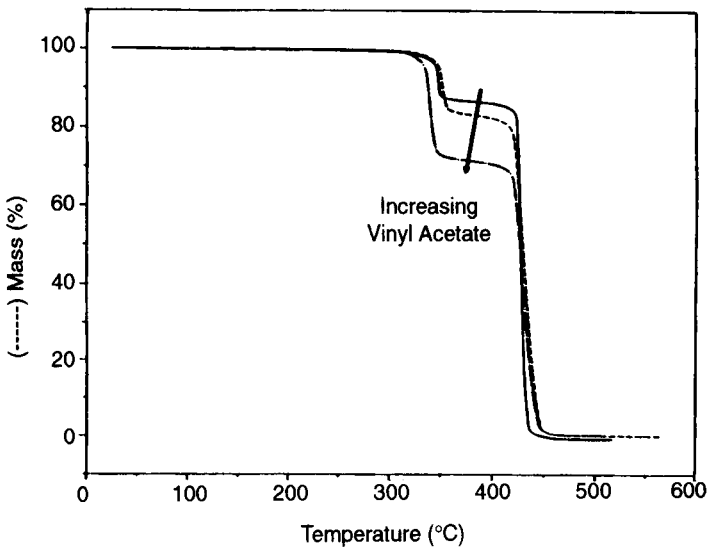

Figure 2.26 Hi-Res™ TGA of ethylene–vinyl acetate copolymer blends. This figure should be compared with Figure 2.20. (Courtesy TA Instruments Ltd.)

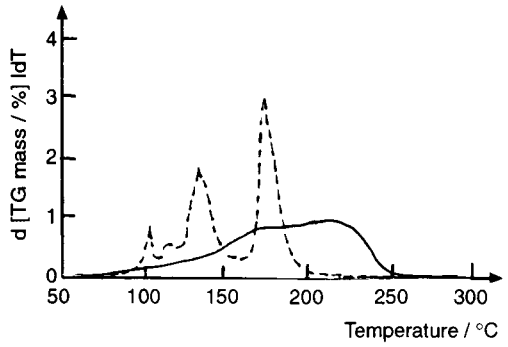

Figure 2.27 Comparison of Hi-Res™ and conventional TG first derivatives for a polymer derivative fuel additive. Solid line, conventional TG; dashed line, Hi-Res™/TG +4.

2.7.2 *Fuel additives*

Fuel and oil additives [77] may be subjected to an oxidative environment and temperatures around 200 °C. They are designed to improve the properties of the oil blend, especially the flow and oxidative stability. Studies of their thermal stability are most important.

Conventional TG of a polymeric derivative used as an additive shows a gradual, poorly differentiated mass loss. Figure 2.27 shows the TG first

derivative curves for conventional and Hi-Res™ TGA of this material. The Hi-Res™ TGA gives a much clearer resolution of the mass losses into three steps, after loss of low-boiling solvent. The mass losses can be quantified more accurately, and the product gases identified by mass spectrometry.

2.7.3 *Drugs*

The presence of water in both 'free' and 'bound' states in pharmaceutical materials is most important. Estimation of the amounts of each type, and the study of water bound in different ways may give better information about the compatibility and action of the drug [78].

Figure 2.28 shows the conventional and Hi-Res™ TGA of a hydrated drug substance, and the DTG curves enable a better separation of the

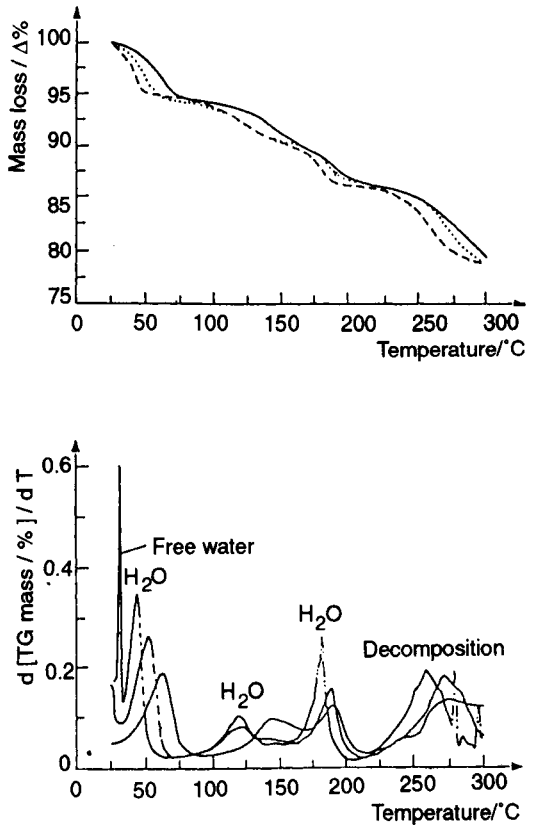

Figure 2.28 Comparison of the Hi-Res™ and conventional TG and DTG of a hydrated drug candidate [78]. Solid line, conventional TG; dotted line, Hi-Res™ index 4; dashed line, Hi-Res™ index 5.

water present in various environments within the material, from the 'free' moisture to two or more kinds of 'bound' water. The trace also shows decomposition at higher temperatures.

2.8 Problems

(Solutions on p. 273)

1. Which of the following physical changes could NOT be detected by thermogravimetry?
   (a) loss of moisture; (b) sublimation; (c) melting; (d) gas adsorption.
2. Which of the following chemical reactions would NOT be detected by thermogravimetry?
   (a) $CaCO_3 + SO_2 = CaSO_4 + CO_2$
   (b) $CaCO_3 + SiO_2 = CaSiO_3 + CO_2$
   (c) $CaCO_3 + Na_2SO_4 = CaSO_4 + Na_2CO_3$
   Calculate the mass change in *any* of the reactions that could be detected.
3. You have decided to investigate a material using thermogravimetry. Make a check-list of all the things you *should* do before attempting to run the sample. If you are investigating the *stability* of the material, what would you do as additional experiments?
4. Magnesium carbonate was dissolved in aqueous oxalic acid and a crystalline product A obtained. When A was heated in air, 9.20 mg of A lost mass in *two* stages only: 2.23 mg were lost up to 220 °C and a further 4.49 mg by 500 °C. Write balanced chemical equations for the preparation and decompositions of A.
5. An alloy containing silver and copper was dissolved in concentrated nitric acid in a small ceramic TG crucible. When heated in air it gave the TG curve of Figure 2.29. Observations showed the residue at the first

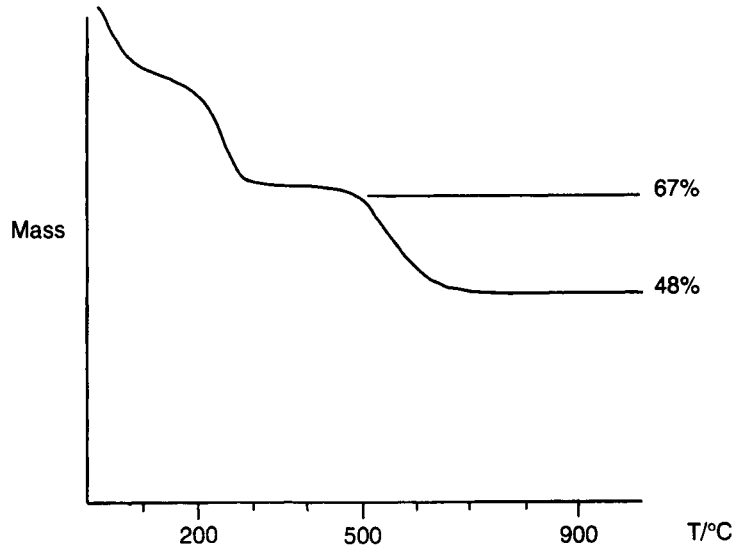

Figure 2.29 TG curve of a silver–copper alloy after solution in nitric acid.

plateau was blue crystals, at the second a black solid and at the third a mixture of black solid and metallic specks. Calculate the percentage silver in the alloy.

6. Using the curves given in Chapter 2 as a guide, sketch the curves for polyethylene (PE) and for poly(vinyl acetate) (PVA). If a copolymer of these two (EVA) loses 15% of its weight in the first stage heating up to 390 °C, calculate the percentage composition of the copolymer.
7. A colleague has performed a series of TG experiments on a sample of a 'pure' substance. He approaches you in some concern, because the results are very different in appearance and in temperatures of the steps. What might he be doing incorrectly? If his results are *correct*, what does this suggest about the sample?

References

1. A.I. Vogel, *Quantitative Inorganic Analysis* (3rd edn), Longman, London, 1961, p. 104.
2. I. Barshad in *Methods of Soil Analysis*, Pt 1, C.A. Black (ed.), No. 9 in Agronomy Series, American Soc. Agronomy, Madison, 1965, Ch. 50.
3. C. Duval, *Inorganic Thermogravimetric Analysis* (2nd edn), Elsevier, Amsterdam, 1963.
4. C.J. Keattch, D. Dollimore, *Introduction to Thermogravimetry*, Heyden, London, 1975, Ch. 1.
5. W. Wendlandt, *J. Chem. Educ.*, 1972, **49**, A571, A623
6. K. Honda, *Sci. Rep. Tohuku Univ.*, 1915, **4**, 97
7. M.I. Pope, M.D. Judd, *Educ. in Chem.*, 1971, **8**, 89
8. P. Chevenard, X. Wache, R. de la Tullaye, *Bull. Soc. Chim. Fr.*, 1944, **10**, 41
9. L. Cahn, H.R. Schultz, *Vacuum Microbalance Techniques*, Vol. 2, Plenum, New York, 1962, p. 7.
10. J.O. Hill, *For Better Thermal Analysis and Calorimetry*, III, ICTAC, 1991.
11. P.D. Garn, O. Menis, H.-G. Wiedemann, *ICTA Magnetic Reference Materials Certificate*, NBS GM-76, 1976.
12. J.M. Thomas, B.R. Williams, *Quart. Rev.*, 1965, **XIX**, 239
13. F.W. Sears, M.W. Zemansky, H.D. Young, *College Physics* (5th edn), Addison Wesley, Reading, MA, 1980.
14. W.L. de Keyser, *Nature*, 1962, **194**, 959.
15. W.-D. Emmerich, E. Kaisersberger, *J. Thermal Anal.*, 1988, **34**, 543; Netzsch TG 439 Brochure, Netzsch Mastermix Ltd.
16. T. Gast, E. Hoinkis, U. Muller, E. Robens, *Thermochim. Acta*, 1988, **134**, 395.
17. Netzsch TG 449 Brochure, Netzsch Mastermix Ltd.
18. E.L. Charsley, A.C.F. Kamp, J.P. Redfern, *Progress in Vacuum Microbalance Techniques*, Vol. 2, eds S.C. Bevan *et al.*, Heyden, London, 1973, p. 97
19. D.A. Skoog, D.M. West, *Fundamentals of Analytical Chemistry* (4th edn), Holt-Saunders, Philadelphia, 1982, Ch. 24.
20. F.W. Fifield, D. Kealey, *Analytical Chemistry* (3rd edn), Blackie, Glasgow, 1990, Ch. 12.
21. F. Brailsford, in *Permanent Magnets and Magnetism*, D. Hadfield (ed.), Iliffe/Wiley, London, 1962.
22. P.K. Gallagher *et al.*, *J. Thermal Anal.*, 1993, **40**, 1423
23. A.R. McGhie, J. Chiu, P.G. Fair, R.L. Blaine, *Thermochim. Acta.*, 1983, **67**, 241
24. E.L. Simons, A.E. Newkirk, *Talanta*, 1964, **11**, 549
25. A.E. Newkirk, *Thermochim. Acta.*, 1971, **2**, 1
26. H.R. Oswald, H.G. Wiedemann, *J. Thermal Anal.*, 1977, **12**, 147
27. P.D. Garn, *Anal. Chem.*, 1961, **33**, 1247
28. M.L. McGlashan, *Physico-Chemical Quantities and Units*, RSC, London, 1968, p. 39.
29. J. Sestak, G. Berggren, *Thermochim. Acta*, 1971, **3**, 1

30. M.E. Brown, D. Dollimore, A.K. Galwey, *Comprehensive Chemical Kinetics*, Vol. 22, *Reactions in the Solid State*, Elsevier, Amsterdam, 1980.
31. M. Reading, D. Dollimore, J. Rouquerol, F. Rouquerol, *J. Thermal Anal.*, 1984, **29**, 775.
32. M. Arnold, G.E. Veress, J. Paulik, F. Paulik, *Thermochim Acta*, 1982, **52**, 67
33. E. Urbanovici, E. Segal, *J. Thermal Anal.*, 1993, **40**, 1321
34. A.K. Galwey, *Thermal Analysis, Proc 7th ICTA*, Wiley, Chichester, 1982, p. 38.
35. K.H. Stern, E.L. Weise, NSRDS-NBS 30: Carbonates, 1969.
36. A. Bhattacharya, *J. Thermal Anal.*, 1993, **40**, 141.
37. J.H. Sharp, G.W. Brindley, B.N.N. Achar, *J. Am. Ceram. Soc.*, 1966, **49**, 379.
38. L.K. Avramov, *Thermochim. Acta*, 1985, **87**, 47.
39. M. Reading, *Thermochim. Acta*, 1988, **135**, 37.
40. C.D. Doyle, *J. Appl. Polym. Sci.*, 1962, **6**, 639.
41. A.W. Coats, J.P. Redfern, *Nature*, 1964, **201**, 68.
42. M.E. Brown, *Introduction to Thermal Analysis*, Chapman & Hall, London, 1988.
43. T. Ozawa, *Bull. Chem. Soc. Japan*, 1965, **38**, 1881.
44. J.H. Flynn, L.A. Wall, *Polym. Lett.*, 1966, **4**, 323.
45. Perkin-Elmer Analytical report, 1985, p. 16.
46. Netzsch Kinetics Software Brochure.
47. J. Rouquerol, *Bull. Soc. Chim. Fr.*, 1964, 31.
48. F. Paulik, J. Paulik, *Anal. Chim. Acta*, 1971, **56**, 328.
49. P.R. Hornsby, C.L. Watson, *Polym. Deg. Stab.*, 1990, **30**, 73.
50. K.A. Broadbent, J. Dollimore, D. Dollimore, *Thermochim. Acta*, 1988, **133**, 131.
51. V.R. Choudhary *et al.*, *Thermochim. Acta*, 1992, **194**, 361.
52. L. Erdey, G. Liptay, G. Svehla, F. Paulik, *Talanta*, 1962, **9**, 489.
53. E.C. Roberson, Stanton Redcroft: Technical Information Sheet, No 18.
54. F. Rodriguez, *Principles of Polymer Systems* (2nd edn), McGraw-Hill, Singapore, 1983, Ch. 11.
55. Stanton Redcroft TG750 Brochure.
56. R.H. Still, *Brit. Polym. J.*, 1979, **11**, 101
57. C.F. Cullis, M.M. Hirschler, *Polymer*, 1983, **24**, 834
58. E.A. Turi, *Thermal Characterisation of Polymeric Materials*, Academic Press, New York, 1981.
59. H.T. Ellingham, *J. Soc. Chem. Ind.*, 1944, **63**, 125
60. D. Dollimore, D.L. Griffiths, D. Nicholson, *J. Chem. Soc.*, 1963, 2617
61. E.L. Charsley, S. St J. Warne, S.B. Warrington, *Thermochim. Acta.*, 1987, **114**, 53.
62. ASTM E1131–86: *Compositional Analysis by Thermogravimetry*, ASTM, Philadelphia, 1986
63. J. Chiu, in *Thermoanalysis of Fibers and Fiber-Forming Polymers*, ed. R.F. Schwenker, Interscience, New York, 1966, p. 25.
64. M. Schnitzer, J.R. Wright, I. Hoffman, *Anal. Chem.*, 1959, **31**, 440.
65. B.D. Mitchell, A.C. Birnie, in *Differential Thermal Analysis*, Vol. 1, ed. R.C. Mackenzie, Academic Press, London, 1970, Ch. 24, p. 695.
66. S. St J. Warne, *Proc 7th ICTA, Toronto*, 1982, Wiley Heyden, Chichester, 1982, p. 1161.
67. C.M. Earnest, R.L. Fyans, *Proc 7th ICTA, Toronto*, 1982, Wiley Heyden, Chichester, 1982, p. 1260; and *Perkin-Elmer Thermal Analysis Application Study*, #32.
68. O. Kubaschewski, B.E. Hopkins, *Oxidation of Metals and Alloys*, Butterworth, London, 1962.
69. B.O. Haglund, *Proc. 1st ESTA, Salford*, 1976, Heyden, London, 1976, p. 415.
70. G. Baran, A.R. McGhie, *Proc 7th ICTA, Toronto*, 1982, Wiley Heyden, Chichester, 1982, p. 120.
71. Y. Shigegaki, S.K. Basu, M. Taniguchi, *Thermochim. Acta*, 1988, **133**, 215.
72. J.P. Chilton, *Principles of Metallic Corrosion*, Royal Society of Chemistry Monographs for Teachers, No 4 (2nd edn), RSC, London, 1973.
73. N. Pernicone, F. Traina, *Pure Appl. Chem.*, 1978, **50**, 1169.
74. S.D. Robertson, B.D. McNicol, J.H. de Baas, S.C. Kloet, J.W. Jenkins, *J. Catal.*, 1975, **37**, 424.
75. J.G. Dunn, Stanton Redcroft Technical Information Sheet, No. 103, 1977.
76. TA Instruments Ltd, TGA 2950 System Brochure.

77. T.J. Lever, A. Sutkowski, *J. Thermal Anal.*, 1993, **40**, 257
78. A.F. Barnes, M.J. Hardy, T.J. Lever, *J. Thermal Anal.*, 1993, **40**, 499.

Bibliography

Note The general thermal analysis texts given at the end of Chapter 1 have substantial sections on thermogravimetry but are *not* listed again here.

C. Duval, *Inorganic Thermogravimetric Analysis* (2nd edn), Elsevier, Amsterdam, 1963.
C.J. Keattch, D Dollimore, *Introduction to Thermogravimetry*, Heyden, London, 1975.